Electrical Engineering
https://doi.org/10.1007/s00202-020-00982-z

ORIGINAL PAPER

Design of measuring and evaluation unit for multi-cell traction battery system of industrial AGV

Michal Frivaldsky[1] · Jozef Sedo[1] · Michal Pipiska[1] · Matus Danko[1]

Received: 28 November 2019 / Accepted: 16 March 2020

Abstract
This paper presents practical design procedure of the electric measuring circuit and evaluation/communication unit of the multi-cell series–parallel connection of traction lead-acid batteries. The target use is online SOC monitoring during the operation of automated guided vehicle (AGV), which is being used for in-house automated industrial processes. Based on the state-of-the-art review, proper methodology for SOC determination was selected for the given lead-acid battery technology. For that purpose, the measuring procedure for identification of the battery equivalent circuit was initially realized and is being described within the main text. The results from the equivalent circuit identification were used for design of the precise measuring circuit which is responsible for the determination of SOC levels based on selected methodologies. These methodologies were implemented within evaluating unit (MCU), while functionality of the proposed system for the SOC identification was tested and evaluated within standard operational conditions of AGV robot.

Keywords State of charge · Estimation · Voltage measurement · Current measurement · Industrial application

1 Introduction

In modern industrial applications, SOC measurements are used by the host systems, for example, to manage power usage and by the application to notify operator about the SOC as battery charge becomes low. This is most important if automated industrial infrastructure is considered, i.e., when mobile industrial robots improve the in-house industrial processes. For such electric vehicles, for example, SOC measurements are essential for estimation of remaining range available to the vehicle for possible operation. In fact, reliable SOC measurement is essential for ensuring safety and maximizing battery life in rechargeable batteries in general and for Li-ion cells. Inaccurate estimation of SOC can result in over-charging and over-discharging, resulting in diminished battery performance and lifetime [1–6].

The battery SOC can be influenced by the battery temperature, the type of battery (lead-acid, Li-ion, LiFePo4, etc.) and the external conditions. Because of these reasons, SOC estimation methods differ from battery applications such as energy storage system, hybrid electric vehicle, electric vehicle or industrial mobile robot [7–11]. Simultaneously, high-power applications like energy storage systems, automotive applications, industrial automated guided vehicles and mobile robots require huge battery modules targeting required voltage for electric drive and for required usable capacity for the active operation [12–14]. In addition to safety and reliability, the battery management electronics are expected to maximize operating range and lifetime, while minimizing cost, size and weight [15–17]. The key elements in the battery management electronics are the battery-monitoring units, which handle a certain number of cells that are clustered in a module. The monitoring unit of each battery module performs the task of accurately measuring voltage, current and temperature of each single cell in the module and transmitting the data to a central battery control unit (BCU) [15–17].

Within this paper, the aim is given on the practical design issues and consequent implementation of the electric measuring circuit and evaluation/communication unit of the multi-cell series–parallel connection of traction lead-acid batteries. The main use of proposed circuit is SOC identification and its monitoring during the operation of automated guided vehicle (AGV), which is being used for in-house automated industrial processes. For this purpose, a proper SOC

✉ Michal Frivaldsky
Michal.frivaldsky@fel.uniza.sk

[1] Department of Mechatronics and Electronics, University of Zilina, Zilina, Slovakia

Published online: 21 March 2020

methodology was selected focusing on the lead-acid battery technology. Identification of the equivalent circuit parameters was realized experimentally, while the results have been used for the design of precise voltage and current measuring circuits. Proposed measuring circuits for series–parallel connection (six cells divided into two strings) were designed and verified by the simulation model as well as by physical prototype. Voltage ratio between battery voltage and measured voltage that was sourced to the evaluating unit (MCU) is the main observed variable. Selected SOC identification methodology was implemented within evaluating unit together with communication protocols for the dispatching system. Proposed SOC identification and evaluation system was finally implemented within AGV, and its functionality was tested and evaluated within standard operational conditions.

2 SOC identification methods for lead-acid traction batteries

Measurement of open-circuit voltage (OCV) can provide sufficiently accurate results but requires special considerations [11]. An open-circuit voltage (OCV) SOC estimation especially works for a lead-acid battery [3, 4]. The use of OCV for SOC estimation can be problematic in dynamic applications where fluctuating load currents result in voltage changes and related diffusion effects (e.g., industrial mobile robots). Therefore, to obtain accurate SOC estimation results, the battery should rest for reaching the equilibrium state of cells before measuring the open-circuit voltage of a battery. When the SOC of a battery is estimated by this method, the state of a battery should be truly in the floating state without the load of battery.

As shown in Fig. 1, the open-circuit voltage method uses the Randles battery model [18] that consists of the cell internal resistance (R_s), the polarization resistance (R_{ct}) and the double-layer capacitance (C_d). A battery OCV in Fig. 1a is a battery terminal voltage when a battery is in the no-load, steady-state condition. Based on the Randles equivalent circuit shown in Fig. 1a, the battery terminal voltage ($V_{terminal}$) can be expressed as:

$$V_{\text{terminal}} = \text{OCV(SOC)} - i\left(R_s + R_{ct}(1 - e^{-t/\tau})\right) \quad (1)$$

where the parameters in (1) can be calculated by τ:

$$R_s = \frac{V_1}{i}, \quad R_{ct} = \frac{V_2}{i}, \quad C_d = \frac{\tau}{R_{ct}} \quad (2)$$

where V_1, V, and τ can be obtained by the time-varying battery terminal voltage shown in Fig. 1b. A battery charge can be expressed as a function of SOC, and therefore the open-circuit voltage method estimates the battery SOC by measuring the OCV and collects data given by (1).

Coulomb-counting method is a common technique for estimation of a battery SOC, while the current from a battery is integrated. However, the problem which decreases the accuracy and robustness of this method is related to the performance of the current sensor and evaluating unit (MCU) that are used, while main limitation is the sampling time during charge or discharge processes of the batteries. Some of the charging units are characterized by the pulse current charging with defined frequency of pulses. If these pulses are too short compared to the sampling performance of used MCU, then the evaluation of SOC will not be accurate enough. On the other side, this estimation method is good for tracking the rapid changes in SOC. Principle of evaluation is described by formula (3).

$$\text{SOC} = \text{SOC}_0 + \frac{1}{C}\int_{t_0}^{t_n} (I_{bat1} - I_{bat0})\mathrm{d}t \quad (3)$$

where C is the rated capacity of battery, I_{bat1} is the battery current and I_{bat0} is the battery current by the loss reactions.

Although each SOC method suffers some limitations, from a practical point of view it is recommended to make a combination of several methods. During fluctuating current or high-current states, the Coulomb-counting method tracks net changes in SOC. During quiet periods, voltage-based methods including OCV measurement help correct errors that accumulated with Coulomb counting.

Both methodologies are combined for the proposed application of SOC estimation of selected battery type (HAWKER NexSys 12 V).

3 Design issues for voltage and current measuring system

Monitoring system is designed for automated guided vehicle (AGV), which is used in industry for transportation of materials or finished products. AGV contains six HAWKER 12XCF158 batteries connected in series–parallel configuration, as shown in Fig. 2, while main electrical–mechanical parameters are listed in Table 1.

The proposed monitoring system provides online measurement (voltage and current every 500 microsecond) of each battery from battery module and consequently estimates actual SOC levels that are sent to the main dispatch unit. Specifications defined by the target application are dependent on AGV parameters, while measuring system shall be adapted to these conditions:

Nominal supply voltage of system 24 V_{dc}

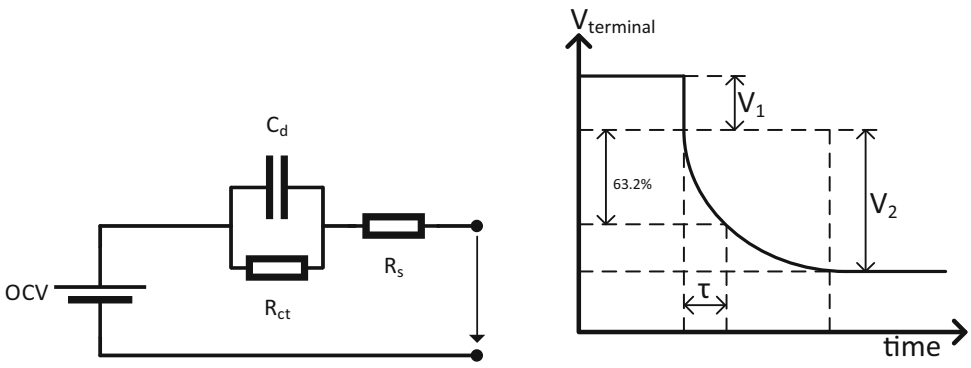

Fig. 1 Equivalent circuit of the Randles battery model (**a**) and the time constant identification during battery discharge (**b**)

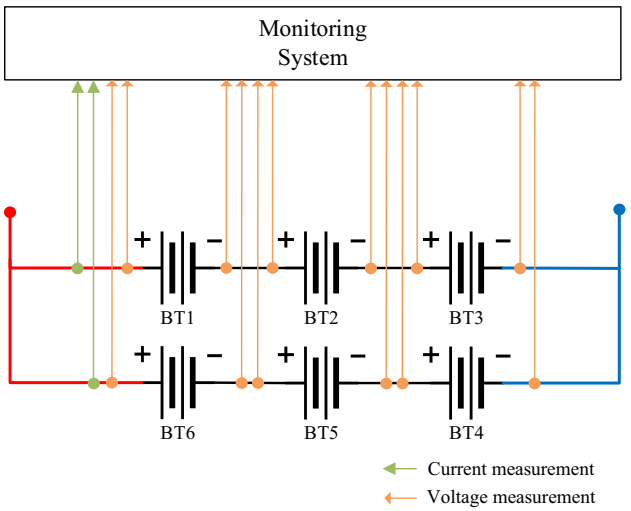

Fig. 2 Block schematic of battery connection and monitoring system with measuring points

Table 1 Hawker 12XCF158 parameters

Nominal voltage (V)	12
Nominal capacity (Ah)	158
Capacity at C1 discharge rate (Ah)	124
Capacity at C3 discharge rate (Ah)	150.6
Capacity at C5 discharge rate (Ah)	158
Length (mm)	561
Width (mm)	125
Height (mm)	283
Weight (kg)	50.8
No. of cycles	1200
Terminal type	M8F
Supply voltage operational range	18–30 V_{dc}
Protections	reverse polarity protection, overcurrent
Measuring voltage range	11–14 V_{dc}
Measuring current range	± 120 A

The measuring circuit can be divided into two individual parts (Fig. 2). The current measurement is responsible for the identification of the amount of charge during discharge and charge processes, while the OCV method is used as secondary supporting method for SOC identification.

The measurement of OCV (Fig. 3) is independent for each of the battery from one leg of the battery module. Individual operational amplifiers are tuned for exact voltage conversion ratio, which is then sourced to the evaluation unit (MCU).

The conversion ratio and its accuracy are defined by the R_4 and R_3 resistors, whose tolerance of the values shall not exceed 1%. The circuit (Fig. 3) is relevant for one battery of the string, and other batteries have the same configuration of the voltage measuring circuit, while the operational amplifiers are tuned for the relevant voltage levels (12 V_{dc}, 24 V_{dc}, 36 V_{dc}). The presented approach can identify voltage values within the range of three decimal points within the range from 11 to 15 V. For that purpose, exact reference (10 V) is being created for each battery. The evaluation unit then recalculates the real OCV value of the battery based on the following equation:

$$V_{\mathrm{BAT\_X}} = 10 + 1.88 \cdot V_{\mathrm{BAT\_X\_OUT}} \tag{4}$$

$V_{\mathrm{BAT\_X}}$, real value of the OCV of battery; $V_{\mathrm{BAT\_X\_OUT}}$, voltage value from differential amplifier.

Approximation is used targeting reduction in the complexity of system. Using this approach, the computation time of this approximation is much smaller than computation with real parameters. This enables to optimize performance of microcontroller.

Figure 4 shows detailed schematic of the used current sensor with filtering components of the measured signal, which is directly sourced to the evaluating unit for the requirements of the use of the Coulomb-counting method. Because the measurements shall be highly accurate, a very precise Hall sensor (L01ZxxxS05 series) was used as main part.

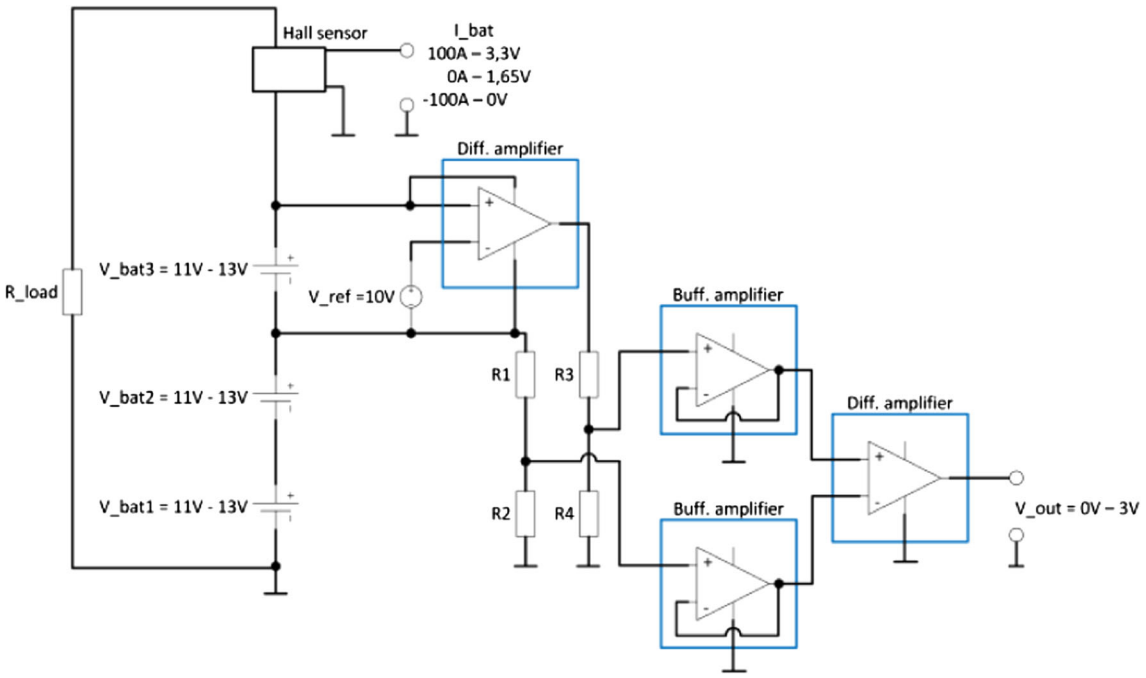

Fig. 3 Block diagram for current and voltage sensing during charging/discharging processes of one battery from battery module

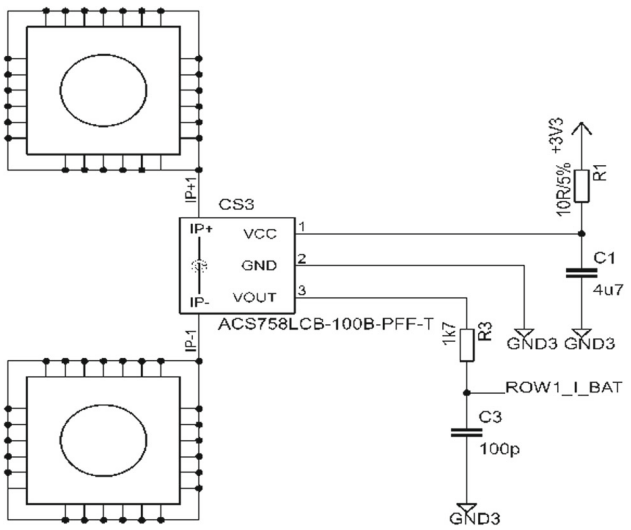

Fig. 4 Measuring circuit for current sensing during charging/discharging processes of the battery

4 Output characteristic measuring procedure of HAWKER 12XCF158 for OCV determination

At this point, the procedure for the identification of the given lead-acid battery output characteristic will be described, whereby focus is given on the determination of OCV versus SOC dependency during defined pulsed charge and discharge cycles. Instead of OCV determination, it is also possible to identify parameters of the equivalent circuit (Fig. 1) in this way [15]. It must be noticed that the investigated battery had 50% of the operational health already passed. It was discovered that OCV versus SOC dependency (considering values) is not even influenced if new, or already cracked, battery is investigated, while the only difference is in the period for which available charge can be utilized.

Experimental assembly is shown in Fig. 5. NI PXI 1031 which contains two PXI 4070 digital multimeters was selected as data logger. The first multimeter is used for direct measure of battery voltage, and the second multimeter measures current in the form of the voltage drop on the shunt resistor, which is used due to the high values of charge and discharge currents. For easy operation of the virtual instruments, the GUI within LabVIEW program was designed for displaying the voltage, current and logging time. Sampling period for data storage of individual variables was set to one second interval.

Initially, the sample of the battery was fully charged and discharged to start the operational–chemical processes of the battery, while experimental test (Fig. 6) stand was realized, according to Fig. 5. The values of battery voltage and current have been sampled each second, while capacity of the current in Ah was calculated.

Consequently, the investigation process was established, which started with charging sequence as follows:

- As charging unit, programmable DC power supply Agilent N8943A was used. It is 500 V–30 A\5000 W (continual power) controlled through LabVIEW instruments.

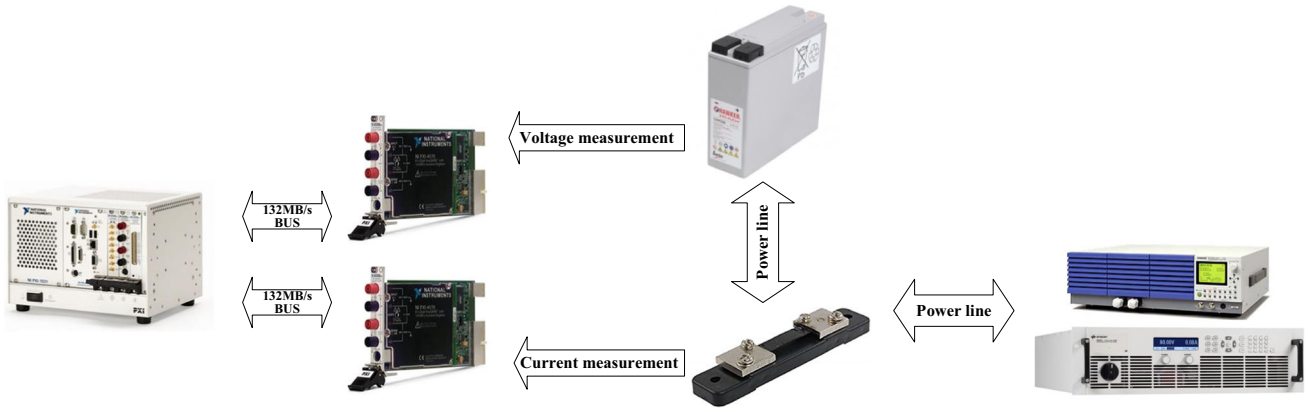

Fig. 5 Principal assembly of experimental test bench for output characteristic measurement of HAWKER 12X CF158 lead-acid battery

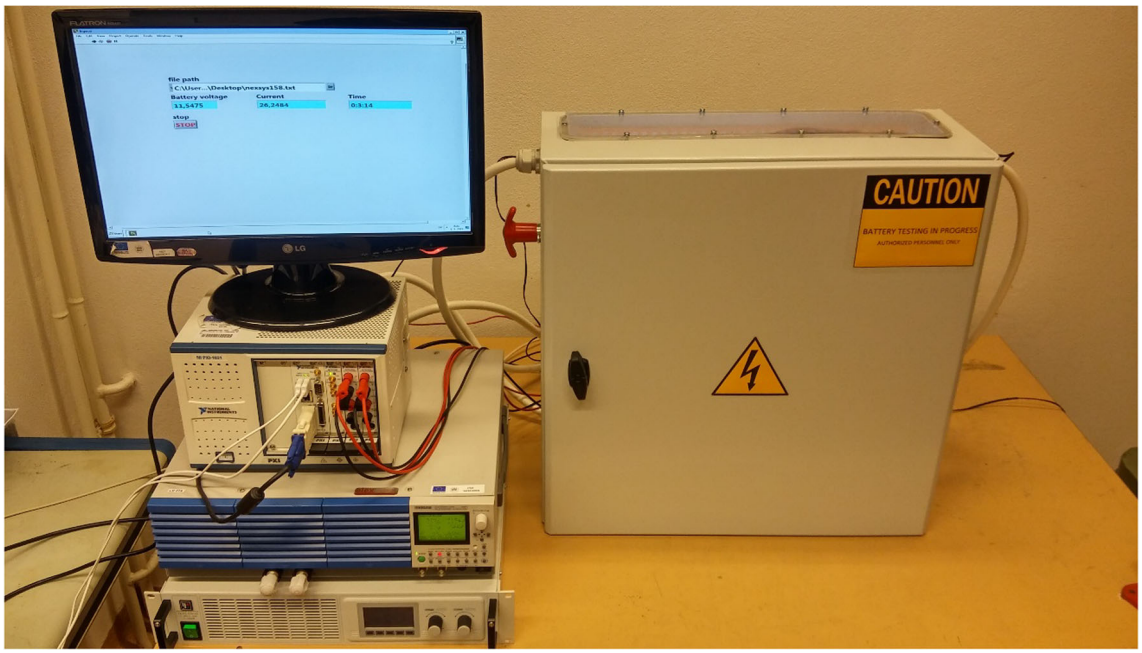

Fig. 6 Experimental test-bench setup for output characteristic measurement of HAWKER 12X CF158 lead-acid battery

- LabVIEW instruments were used for program operation which secures counting of the charging current Ah, while after each 10 Ah what is 10% of nominal capacity, the charging process was stopped to observe OCV. After 5-min pause (recovery of battery terminal voltage), power supply was again connected to continue charging process. Whole sequence has finished after 156 Ah was counted, which corresponds to the nominal capacity of the battery.

After charging process has been finished, discharging procedure was realized similarly, whereby electronic load Kikusui PLZ1004W was controlled as follows:

- A discharging current is monitored and counted, while after each 10 Ah discharging is stopped and 5 min of battery regeneration is provided. Whole discharge process has finished after discharge of 156 Ah, thus after battery full discharge.

Diagram for the initialization as well as for the testing procedure based on the previous description is shown in Fig. 7.

5 Analysis of the acquired data for output characteristic determination

Figure 8 shows acquired output characteristic of the investigated lead-acid battery, where battery voltage during charging\discharging is evaluated in dependency on SOC. Both charging and discharging states are being shown. The rest-

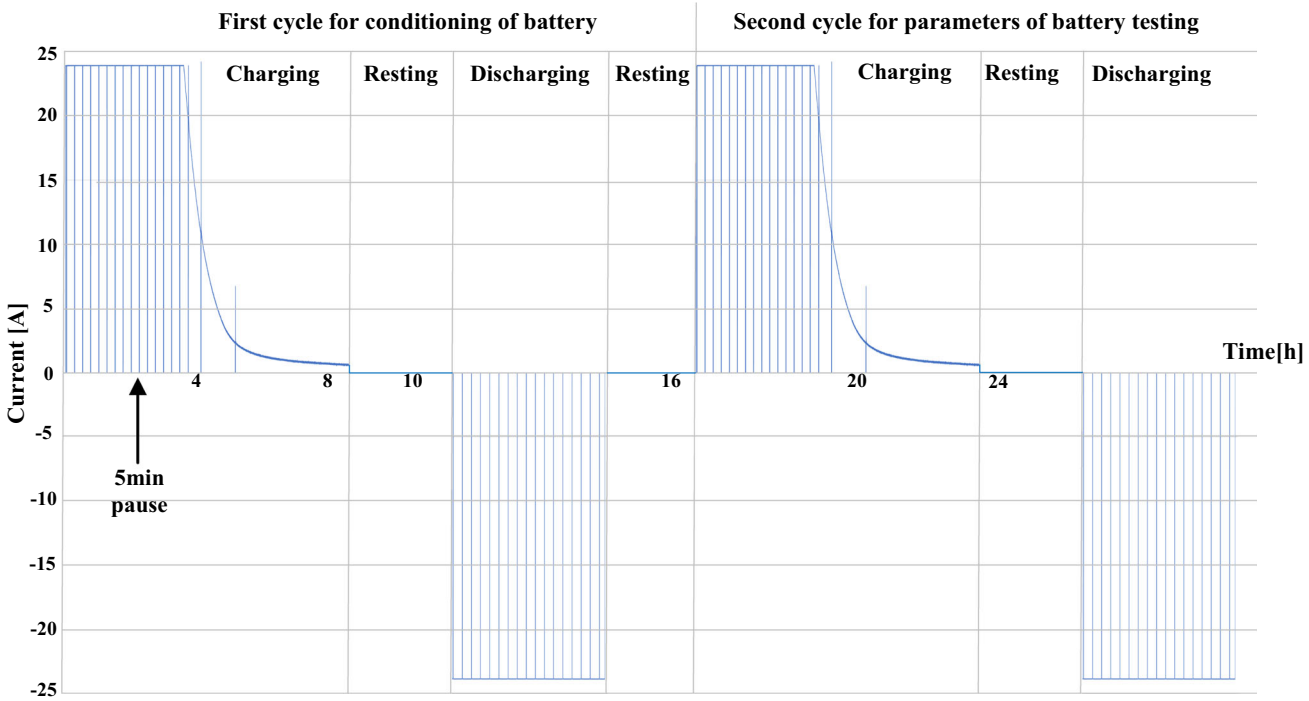

Fig. 7 Charging and discharging diagram of the procedure for the output characteristic determination

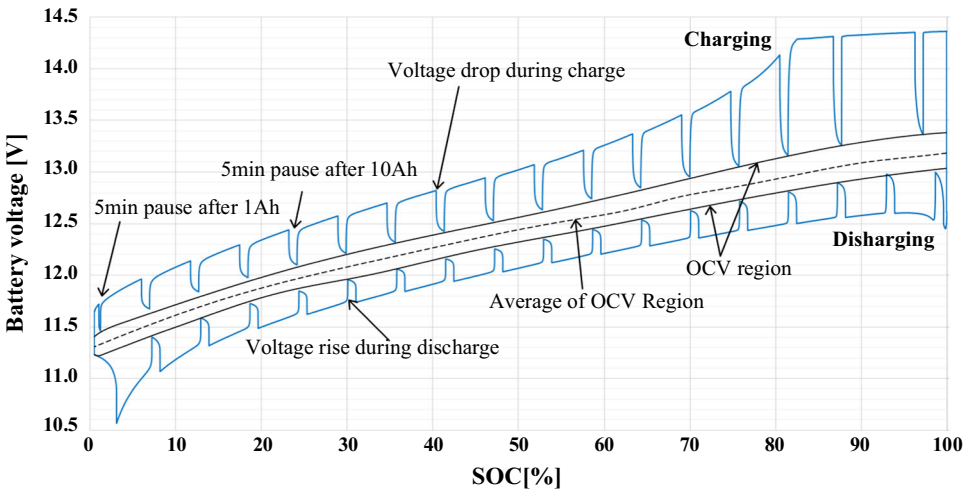

Fig. 8 Measured output characteristic (OCV vs. SOC) of HAWKER 12XCF158 acquired by test procedure from Fig. 7

ing periods are characterized by the OCV regeneration. (For charging procedure, OCV decreases, and for the discharging procedure OCV increases). For both sequences, the regions with the steady states of OCV are connected by the solid lines. These values are considered as reference intervals of maximum and minimum of OCV, while mean value (dashed line) is evaluated as OCV parameter for SOC estimation by OCV method. The reason why average value of OCV is considered is related to the battery regeneration abilities, which shall be higher than 5-min regeneration intervals (several hours) in order to achieve averaged values V_0, V_1, V_2 and V_3 (Fig. 9).

V_0 is voltage during discharge, after load is switched off, voltage is almost immediately increased to level V_1. Voltage further rises exponentially, and maximum curve fit of this voltage is V_2. V_3 is level of voltage after load is switched on again.

Table 2 shows extracted values of the OCV for SOC identification, while these values will be further used for the implementation within measuring and evaluation unit of the proposed SOC monitoring system of AGV robot.

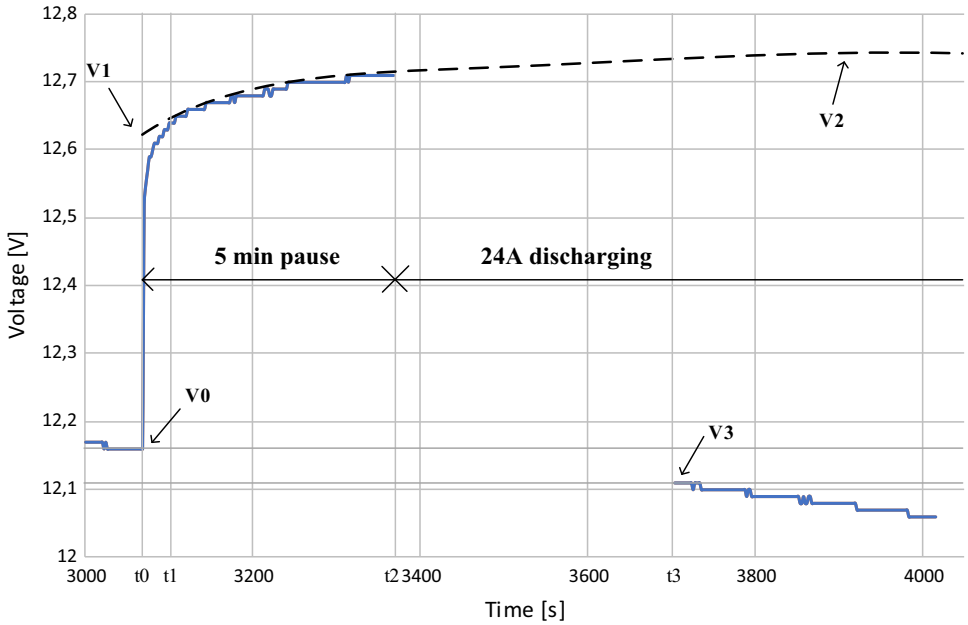

Fig. 9 Regeneration period during battery regeneration (discharging sequence)

Table 2 OCV versus SOC

SOC (%)	100	90	80	70	60	50	40	30	20	10
OCV (V)	13.188	13.036	12.87	12.69	12.496	12.288	12.066	11.83	11.58	11.316

6 Experimental verification of measuring system

The verification of the proposed circuit was initially done by the simulation in MATLAB SIMULINK (Fig. 10). The battery module is modeled by the equivalent voltage sources which reflect the OCV of the measured battery. The main investigated variable was the voltage conversion ratio, which is important for evaluating unit.

Table 2 shows extracted values of the OCV for SOC identification, while these values will be further used for the implementation within measuring and evaluation unit of proposed SOC monitoring system of AGV robot.

Table 3 shows numerical results from the simulation experiment, whereby the procedure was as follows:

- OCV of each battery (V_{BAT1}–V_{BAT3}) was varying from its upper level (15 V)—V_{BAT} to its bottom level (11 V).
- The values which lie between these values and are estimated by (X) are relevant for SOC estimation. The conversion ratio for individual cells is the same, and voltages U_{OUT1}–U_{OUT3} are supplied to the evaluation MCU.

Experimental verification was realized similar to the simulation. The OCV was emulated by the adjustable voltage sources, while the value was changed from top to the bottom value of the battery. Table 3 shows also numerical results from the experimental measurement. Results show minimal difference between simulation results and experimental measurements. The evaluated relative error is within the whole measured range for each battery (Table 4). Experimental circuit is shown in Fig. 11, while it is valid for the one battery of the series string.

$$\text{Rel\_Error} = \frac{U_{BAT\_MEAS} - U_{BAT\_SIM}}{U_{BAT\_MEAS}} \quad (5)$$

Results show minimal difference between simulation results and experimental measurements. The evaluated relative error is within the whole measured range for each battery. It is seen (Table 3) that its value varies from − 7% from its maximum to 0% at minimum. The highest error is presented for the top battery from series connection of the module. This highest deviation is related to the requirement on the most precise setting of OP AMPs, which for this part of module converts the highest voltage of the battery module, thus it is connected at the highest potential. Anyway it can be said that the proposed measuring circuit for OCV evaluation has expected accuracy and functionality and might be used for the target application, which is SOC estimation of the considered battery module.

7 Evaluation and dispatching unit

The main part of the evaluation system is processor TI-C2000 family which is responsible for all calculations, estimations,

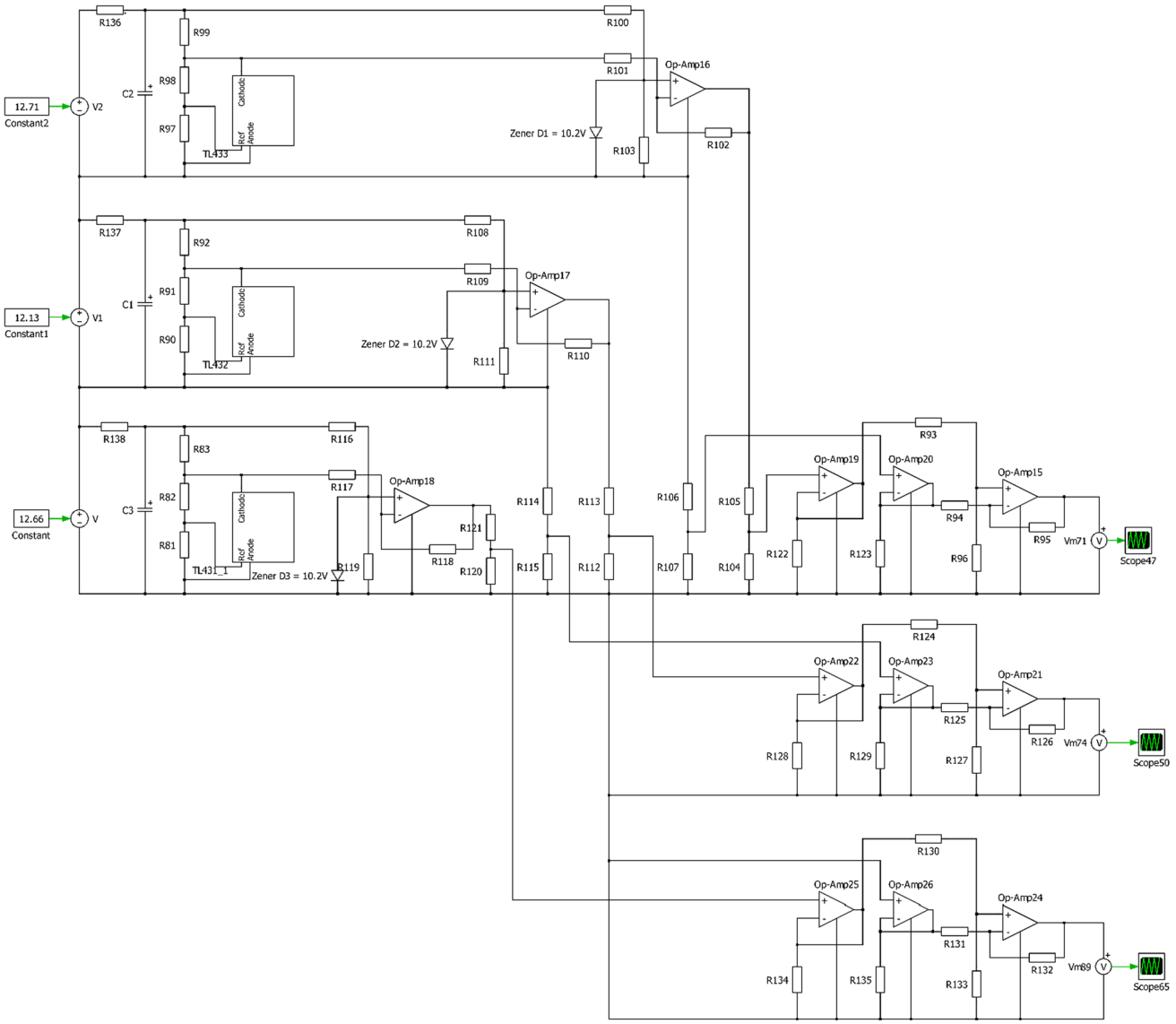

Fig. 10 Simulation model of the measuring circuit for voltage sensing

communication and data transfer to dispatching system of the factory. The main principle of evaluation is related to the requirements on the proper sampling and calculation of the current to achieve accurate and relevant results. As was already mentioned a very precise Hall sensor was used for this purpose.

The sampling frequency is 2 kHz ($T_s = 0.5$ ms). The converter is 12-bit with two sample-and-hold units. Each 0.5 ms, it measures the voltage on each battery and the value of the current of battery series string, i.e., six voltages and two currents are being monitored. From these values, the integral values are being calculated with the use of trapezoidal method:

$$i_{int}[0] = i_{int}[1] + \frac{i[0] + i[1]}{2} T_s \tag{6}$$

$i_{\text{int}}[0]$, actual value of the integral of current; $i_{\text{int}}[1]$, previous value of the integral of current, i.e., the value of one sample before; $i[0]$, actual value of the measured current; $i[1]$, previous value of the measured current; T_s, sampling period 0.5 ms.

Subsequently, every 5 s from the integral values, the mean values of the voltages and currents are estimated. For this purpose, the individual integrals are divided by the value of period $T = 5$ s. When the measurement is started, the initial SOC value is estimated from the value of the voltage OCV, according to Table 1. Linear interpolation between table values is being used during evaluation. If the battery is loaded, the no-load voltage is estimated as the voltage on the battery plus the voltage drop on the internal battery resistance (value identified by the experimental measurements). After initial

Table 3 Comparisons of the simulated and measured values within the range of batteries sensed voltages

Simulation results						Real measurement						
U_{BAT1} (V)	U_{OUT1} (V)	U_{BAT2} (V)	U_{OUT2} (V)	U_{BAT3} (V)	U_{OUT3} (V)	U_{BAT1} (V)	U_{OUT1} (V)	U_{BAT2} (V)	U_{OUT2} (V)	U_{BAT3} (V)	U_{OUT3} (V)	Nr.
11	0.5239	11	0.5242	11	0.5244	11.004	0.488	11.015	0.534	11.017	0.53	1
11.5	0.7911	11.5	0.7915	11.5	0.7918	11.503	0.752	11.497	0.795	11.507	0.789	2
12	1.0584	12	1.0589	12	1.0592	12.002	1.017	11.992	1.055	12.004	1.053	3
12.5	1.3256	12.5	1.3262	12.5	1.3266	12.502	1.282	12.514	1.334	12.506	1.319	4
13	1.5928	13	1.5936	13	1.5941	13.002	1.547	13.048	1.619	12.996	1.579	5
13.5	1.86	13.5	1.8609	13.5	1.8615	13.499	1.809	13.52	1.871	13.494	1.846	6
14	2.1272	14	2.1282	14	2.1289	14	2.075	14	2.127	14.042	2.138	7
14.5	2.3944	14.5	2.3956	14.5	2.3963	14.502	2.341	14.502	2.394	14.522	2.395	8
15	2.6615	15	2.663	15	2.6638	15	2.605	15.055	2.687	15.017	2.659	9

determination of SOC, the other SOC values are determined by the use of Coulomb counting:

$$\mathrm{SOC}[0] = \mathrm{SOC}[1] + \frac{i_{\mathrm{int}}[0]}{C} \tag{7}$$

SOC[0], actual value of SOC; SOC[1], previous value of SOC (initial state taken from the table values of OCV); $i_{\mathrm{int}}[0]$, actual value of the integral current; *C*, nominal capacity of accumulator.

After SOC estimation, the measured and calculated values are filled into packets, control sum CRC is evaluated

Table 4 Evaluation of the relative error between measurement and simulation

Relative error evaluation									
U_{OUT_REL1}	− 7%	− 5%	− 4%	− 3%	− 3%	− 3%	− 3%	− 2%	− 2%
U_{OUT_REL2}	2%	0%	0%	1%	2%	1%	0%	0%	1%
U_{OUT_REL3}	1%	0%	− 1%	− 1%	− 1%	− 1%	0%	0%	0%
Nr.	1	2	3	4	5	6	7	8	9

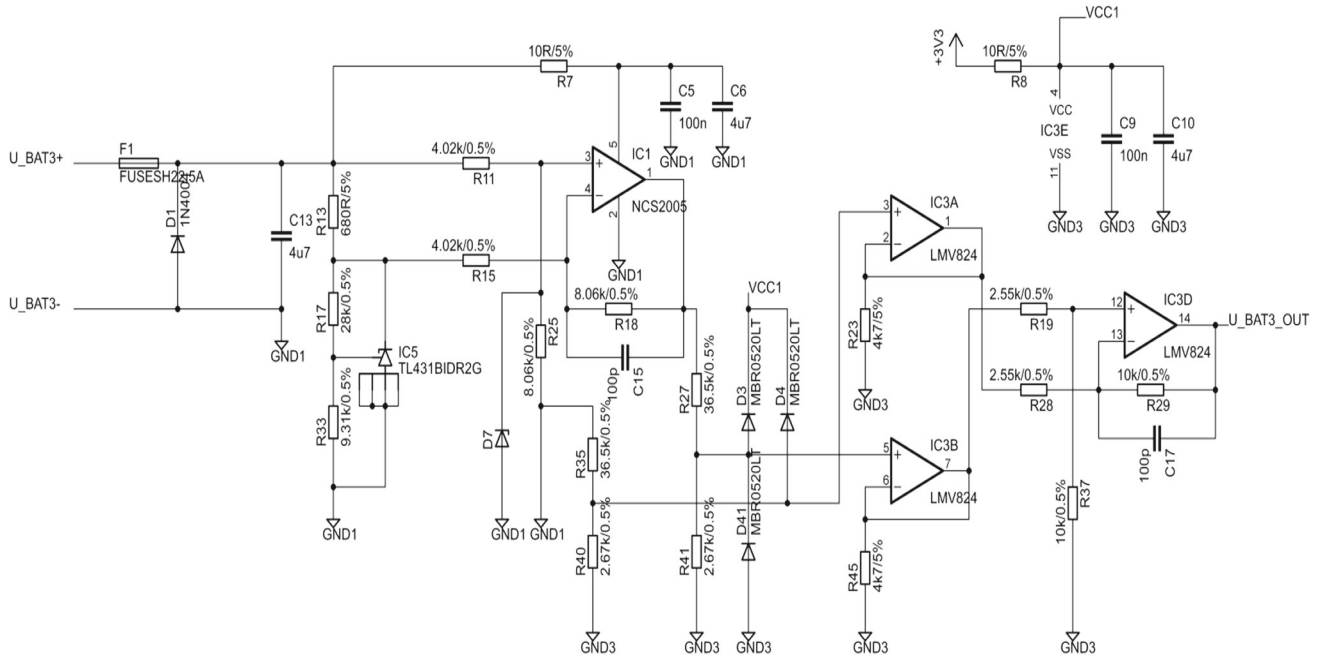

Fig. 11 Schematic of measuring circuit for OCV voltage sensing for one battery from the battery module

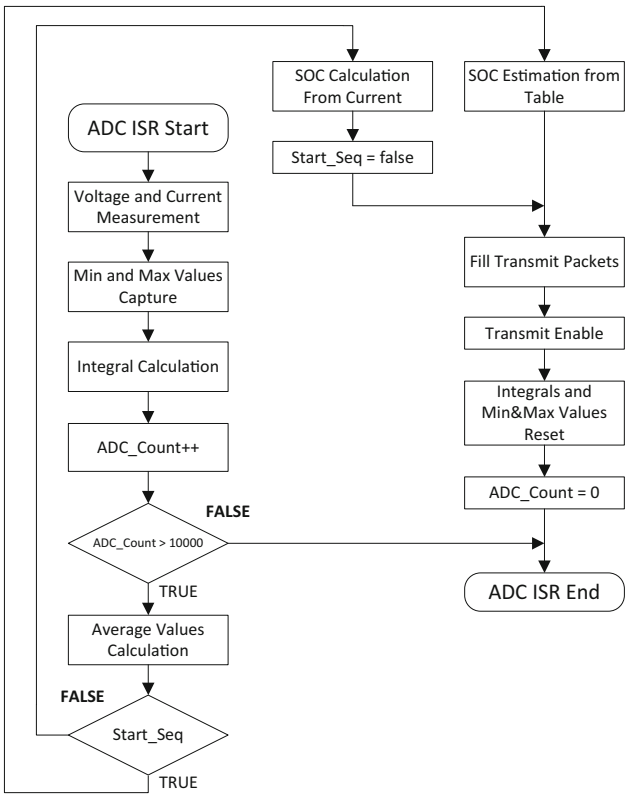

Fig. 12 Evaluation algorithm of the SOC estimation and data transfer

and consequently these packets are sent through series link into UART of the Ethernet module Waveshare 12,161, which serves as client and communicates with supervising system (Fig. 12).

8 Verification of proposed SOC identification system within standard operational conditions of AGV robot

Figure 13 shows practical realization of the proposed SOC evaluation system, which can be divided into two parts, e.g., measuring unit and evaluation unit. Both segments have been initially verified from the functional point of view (previous chapter). The implementation of this unit was performed for the mentioned AGV, while battery module from Fig. 2 was monitored and represents traction energy storage system.

The verification of the design proposal of the SOC identification system for custom AGV robot application was realized within the operational conditions, which are relevant for standard daily operation of the AGV machine. Tests have been performed within verification laboratory, where AGV was running through predefined area that reflects the operational characteristic within industrial factory. Procedure is divided into two parts, i.e., discharging sequence, which reflects the operation of the AGV and then charging sequence, which reflects the requirement of the energy delivery after AGV finishes its operation.

8.1 Discharging procedure of SOC estimation within AGV operation

The discharging sequence was lasting approximately for 3 h (10,683 s) during which AGV performed standard operational actions.

Figure 14 shows time dependency of the OCV voltage of individual battery cells of the module. Figure 14 shows the regeneration intervals, which have been caused by the short-time charge within the charging station of AGV. These stations are located within operation route of the AGV, while short-time charge shall prolong operational radius.

Figure 15 shows time dependency of the SOC estimation based on the actual information of the OCV value and amount of the charge taken during AGV operation. SOC of individual batteries is uneven, which reflects the actual value of the battery voltage. In principle, the SOC values after 3 h of the AGV operation decrease to the app. 50% of the battery's capacity. It is seen in the time 7000 s that there is small increase in the SOC which is caused by mentioned short-charge cycle.

8.2 Charging procedure of SOC estimation within AGV operation

When the discharging procedure relevant for the AGV operation has finished, it was considered that the charging process will start. Within real conditions, the full charge of individual AGV is required; thus, charging process was lasting for the period required for full batteries charge. Figure 16 shows time dependency of the charging currents relevant for two parallel strings of battery module.

The charging sequence was provided by the charging unit that is originally suited for the given battery technology. With the rise of the battery voltages, charging current decreases continually. SOC values have reached maximal values (Fig. 17) at the end of the charging process. It is seen that the full SOC was achieved for five of the six batteries. The difference in the one of the batteries is evident and is caused due to aging effects.

9 Conclusions

The presented paper has shown possible approach for design of the electronic measuring circuit for OCV (open-circuit voltage) which is suitable for the SOC estimation of lead-acid traction battery module. Measuring circuit presents interface between measured component and evaluating unit. Evaluation unit is responsible for the determination of current

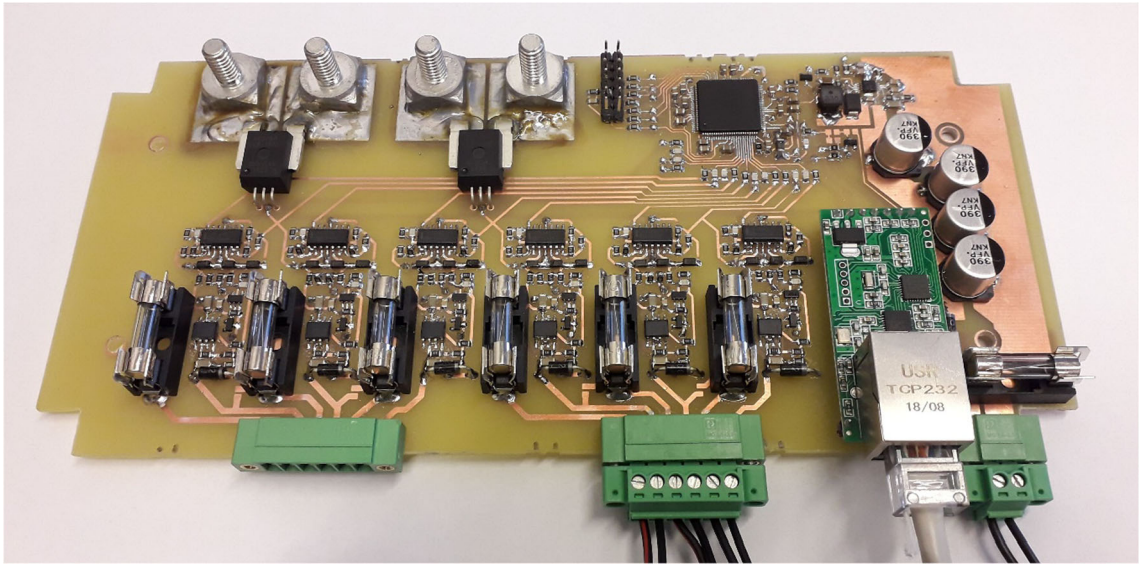

Fig. 13 Practical realization of measuring and communication unit for AGV machine SOC estimation

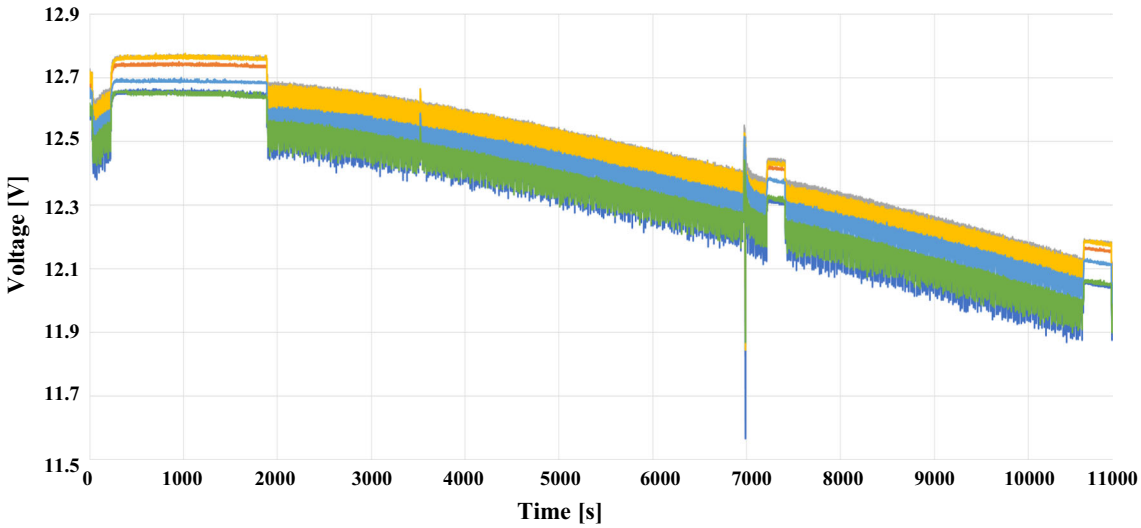

Fig. 14 Time dependency of the OCV voltages on the individual batteries of the AGV battery module during robot operation

SOC value, which is being determined based on combination of OCV method and Coulomb-counting method, which are implemented within evaluation processor. Important parameter for the determination of OCV was precise voltage measurement of the series connection of three batteries and relevant conversion voltage ratio between individual battery voltage and output voltage sourced to the evaluating processor. Main outcome is based on the proposal, which utilizes cascade connection of operational amplifier. Each cell of the battery module has its own measuring channel. The proposal was evaluated by the simulation analysis first where proper functionality and component calculation were confirmed. Consequently, practical design was realized and verified. Experimental measurements have showed that the difference between expected (simulation) and real (measurements) behaviors varies within the range of the relative error in interval (− 7 to 0%). The highest deviation was found for the top cell connected at the highest potential of series batteries connection. Due to this fact, the proposed system has to converter higher voltage for this battery with lower accuracy compared to the others. The performance and evaluation of the system were consequently tested at practical application during standard operation of AGV robot. Requirement on the online monitoring of SOC was secured by the communication and evaluation unit, which also provide data transfer to the dispatching system. It was found that the measuring system provides its required performance, and SOC identification was verified during charging and discharging process,

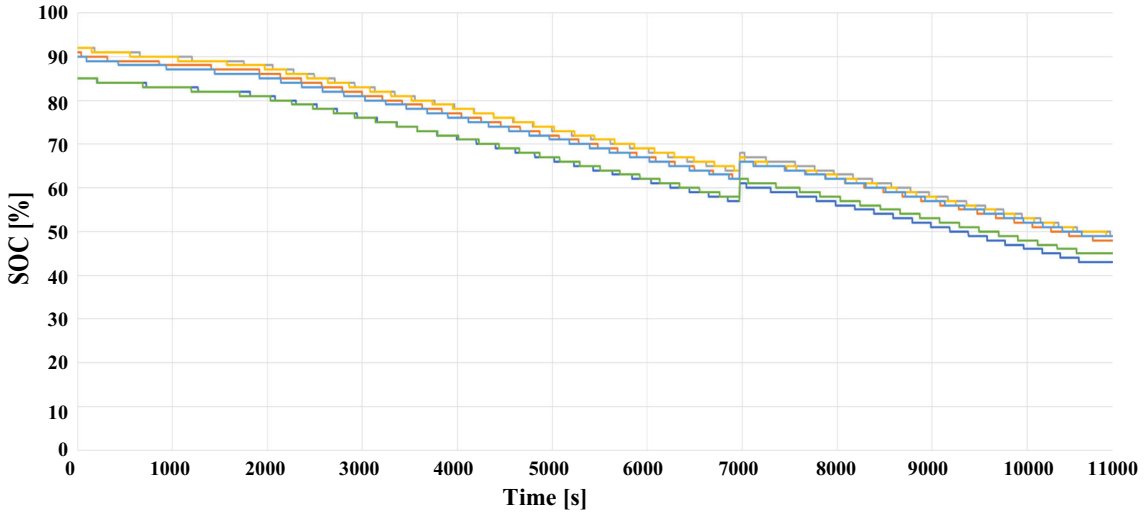

Fig. 15 Time dependency of SOC of individual batteries during AGV robot operation

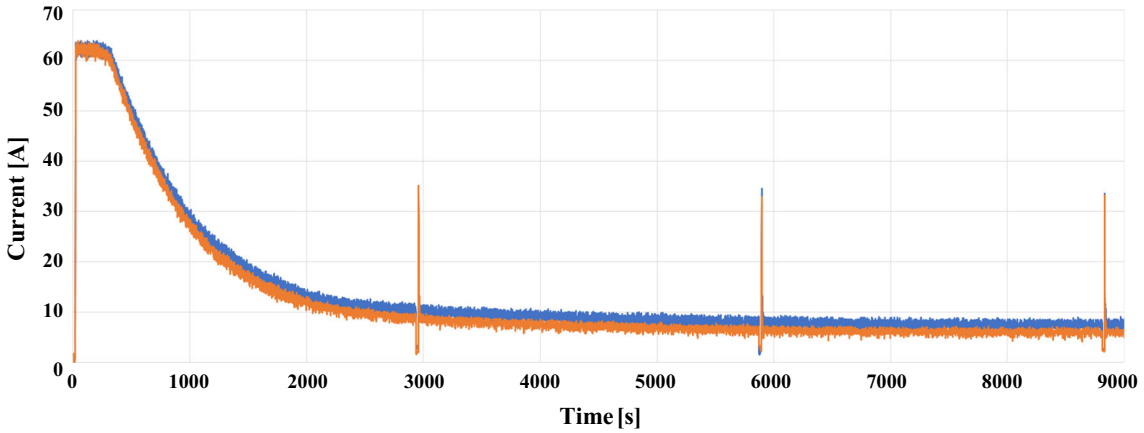

Fig. 16 Time dependency of the battery module charging current of the AGV battery module during robot operation

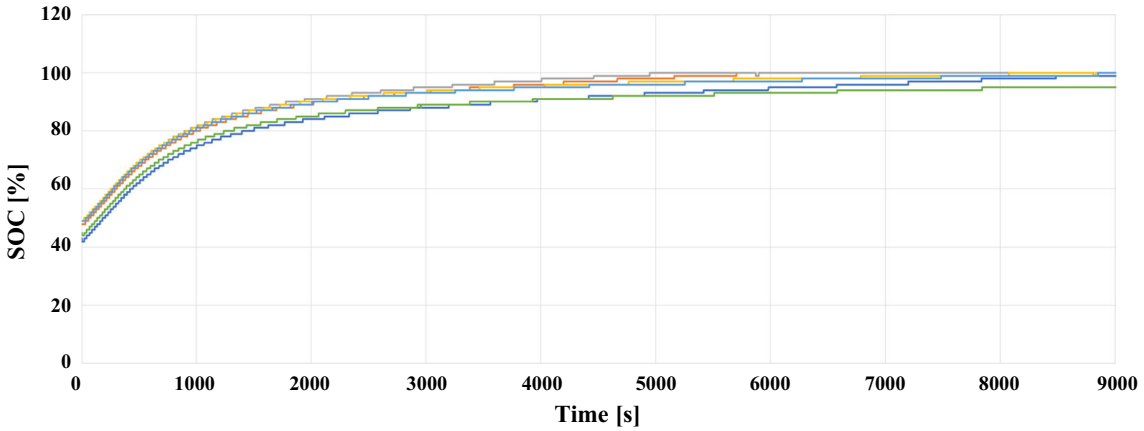

Fig. 17 Time dependency of SOC of individual batteries during AGV robot charging

thus the proposed system is suitable for the practical application within relevant field (in-house industrial automated processes).

Acknowledgements This research was funded by a Grant (No. APVV-15/0396 and APVV-17/0345) from the Agentura na podporu vyskumu a vyvoja, Slovakia, and by a Grant (No. Vega-1/0547/18).

References

1. Prochazka P, Knobloch J, Cervinka D, Kadlec J, Cipin R, Pazdera I (2014) Communication and energy management system of small electric airplane. In: Proceedings of the 16th international conference on mechatronics—mechatronika 2014, Brno, pp 11–15. https://doi.org/10.1109/mechatronika.2014.7018229
2. Dai X, Zhang C, Li S, Zhou W (2010) State monitor for lithium-ion power battery pack. In: 2010 International conference on measuring technology and mechatronics automation, Changsha City, pp 481–484. https://doi.org/10.1109/icmtma.2010.81
3. Ouannes I, Nickel P, Dostert K (2014) Cell-wise monitoring of lithium-ion batteries for automotive traction applications by using power line communication: battery modeling and channel characterization. In: 18th IEEE international symposium on power line communications and its applications, Glasgow, pp 24–29. https://doi.org/10.1109/isplc.2014.6812322
4. Liu Z, Li Z, Zhang J, Su L, Ge H (2019) Accurate and efficient estimation of lithium-ion battery state of charge with alternate adaptive extended Kalman filter and Ampere-hour counting methods. Energies 12:757
5. Omar N, Daowd M, Hegazy O, Mulder G, Timmermans J-M, Coosemans T, Van den Bossche P, Van Mierlo J (2012) Standardization work for BEV and HEV applications: critical appraisal of recent traction battery documents. Energies 5:138–156
6. Zhang R, Xia B, Li B, Cao L, Lai Y, Zheng W, Wang H, Wang W (1820) State of the art of lithium-ion battery SOC estimation for electrical vehicles. Energies 2018:11
7. Gao J, Zhang Y, He H (2015) A real-time joint estimator for model parameters and state of charge of lithium-ion batteries in electric vehicles. Energies 8:8594–8612
8. Sabatiera J, Aouna M, Oustaloupa A, Grégoireb G, Ragotb F, Royb P (2006) Fractional system identification for lead acid battery state of charge estimation. Sig Process 86(10):2645–2657. https://doi.org/10.1016/j.sigpro.2006.02.030
9. Nobile G, Cacciato M, Scarcella G, Scelba G (2018) Multi-criteria experimental comparison of batteries circuital models for automotive applications. Communications 20(1):97–104
10. Cai C, Du D, Liu Z, Ge J (2002) State-of-charge (SOC) estimation of high power Ni-Mh rechargeable battery with artificial neural network. In: Proceedings of the 9th international conference on neural information processing (ICONIP'OZ). https://doi.org/10.1109/iconip.2002.1198174
11. Piller S, Perrin M, Jossen A (2011) Methods for state-of-charge determination and their applications. J Power Sources 96:113–120. https://doi.org/10.1016/S0378-7753(01),00560-2
12. Aiello G, Cacciato M, Messina S, Torrisi M (2018) A high efficiency interleaved PFC front–end converter for EV battery charger. Communications 20(1):86–91
13. Rodriguesa S, Munichandraiahb N, Shuklaa AK (2000) A review of state-of-charge indication of batteries by means of A.C. impedance measurements. J Power Sources 87:12–20. https://doi.org/10.1016/s0378-7753(99)00351-1
14. Bayir R, Soylu E (2018) Real time determination of rechargeable batteries' type and the state of charge via cascade correlation neural network. Elektronika IR Elektrotechnika. https://doi.org/10.5755/j01.eie.24.1.20150
15. Huet F (1998) A review of impedance measurements for determination of the state-of-charge or state-of-health of secondary batteries. J Power Sources 70:59–69. https://doi.org/10.1016/S0378-7753(97),02665-7
16. Galád M, Špánik P, Cacciato M et al (2017) The SOC estimation of a lead acid rechargeable battery. Electr Eng 99:1233. https://doi.org/10.1007/s00202-017-0618-z
17. Galád M, Špánik P, Cacciato M, Nobile G (2016) Comparison of common and combined state of charge estimation methods for VRLA batteries. In: 2016 ELEKTRO, Strbske Pleso, pp 220–225. https://doi.org/10.1109/ELEKTRO.2016.7512069
18. Turgut M, Bayir R, Duran F (2018) CAN communication based modular type battery management system for electric vehicles. Elektronika IR Elektrotechnika. https://doi.org/10.5755/j01.eie.24.3.20975